

## Contamination of Sunyaev-Zel'dovich Clusters in AMiBA Observations

Guo-Chin Liu<sup>1,2</sup>, Mark Birkinshaw<sup>3</sup>, Jiun-Huei Protty Wu<sup>5</sup>, Paul T. P. Ho<sup>1,4</sup>, Chih-Wei Locutus Huang<sup>5</sup>, Yu-Wei Liao<sup>5</sup>, Kai-Yang Lin<sup>1,5</sup>, Sandor M. Molnar<sup>1</sup>, Hiroaki Nishioka<sup>1</sup>, Patrick M. Koch<sup>1</sup>, Keiichi Umetsu<sup>1</sup>, Fu-Cheng Wang<sup>5</sup>, Pablo Altamirano<sup>1</sup>, Chia-Hao Chang<sup>1</sup>, Shu-Hao Chang<sup>1</sup>, Su-Wei Chang<sup>1</sup>, Ming-Tang Chen<sup>1</sup>, Chih-Chiang Han<sup>1</sup>, Yau-De Huang<sup>1</sup>, Yuh-Jing Hwang<sup>1</sup>, Homin Jiang<sup>1</sup>, Michael Kesteven<sup>6</sup>, Derek Kubo<sup>1</sup>, Chao-Te Li<sup>1</sup>, Pierri Martin-Cocher<sup>1</sup>, Peter Oshiro<sup>1</sup>, Philippe Raffin<sup>1</sup>, Tashun Wei<sup>1</sup>, Warwick Wilson<sup>6</sup>

### ABSTRACT

We investigate the contamination of the Sunyaev-Zel'dovich effect for six galaxy clusters, A1689, A1995, A2142, A2163, A2261, and A2390, observed by the Y. T. Lee Array for Microwave Background Anisotropy (AMiBA) during 2007. With the range of baselines used, we find that the largest effect (of order 13-50% of central SZ flux density) comes from primary anisotropies in the Cosmic Microwave Background, which exceeds the thermal noise in all six cases. Contamination from discrete radio sources is estimated to be at a level of 3-60 %. We use the statistics of these contaminating sources to estimate and correct the errors in the measured Sunyaev-Zel'dovich effects of these clusters.

*Subject headings:* cosmology: observations – diffuse radiation: galaxy clusters: general — individual clusters, SZE observation

### 1. Introduction

Measurements of the Sunyaev-Zel'dovich effect (Sunyaev & Zel'dovich 1972, SZE) are contaminated by foregrounds and backgrounds at a level that depends on the angular scale of interest and

---

<sup>1</sup>Academia Sinica, Institute of Astronomy and Astrophysics, P.O.Box 23-141, Taipei 106, Taiwan

<sup>2</sup>Department of Physics, Tamkang University, 251-37 Tamsui, Taipei County, Taiwan

<sup>3</sup>Department of Physics, University of Bristol, Tyndall Ave, Bristol, BS8 1TL, UK

<sup>4</sup>Harvard-Smithsonian Center for Astrophysics, 60 Garden Street, Cambridge, MA 02138, USA

<sup>5</sup>Department of Physics, Institute of Astrophysics, & Center for Theoretical Sciences, National Taiwan University, Taipei 10617, Taiwan

<sup>6</sup>Australia Telescope National Facility, P.O.Box 76, Epping NSW 1710, Australia

the frequency of observation. Primary anisotropies in the Cosmic Microwave Background (CMB) from redshift  $z \simeq 1100$  dominate on scales larger than a few arcmin ( $\ell \lesssim 2000$ ) but have a spectrum that differs significantly from the SZE, and so can be removed by multi-wavelength observations. Galactic contamination arises from synchrotron, free-free, and dust emission and can also affect SZE measurements. Synchrotron and free-free emission usually dominate at low radio frequencies, while dust emission is most important at mm and submm wavelengths, with a crossover frequency of 60 – 70 GHz. Emission from discrete radio sources is less important at high radio frequencies, but can be problematic even at 90 GHz. Spatial filtering, by observing at a finer angular resolution than the scale of the SZE, can mitigate this problem. Finally, SZE data are commonly affected by the pickup of signals from the ground, the atmosphere, and other local emitters, which have to be carefully corrected for or avoided.

AMiBA (Ho et al. 2009; Chen et al. 2009; Koch et al. 2009a; Wu et al. 2009) will be subject to all these issues. AMiBA was designed to operate from 86 – 102 GHz and to be sensitive to multipoles  $800 \lesssim \ell \lesssim 2600$ . The observing frequency was chosen to minimize contamination from non-SZE effects while working within a window of good atmospheric transmission. It is generally assumed that radio source contamination is less of a problem for AMiBA than for other instruments that operate at lower frequencies. However, sources with inverted spectra may still cause difficulties, so it is important to consider the radio environment for any AMiBA field. The level of CMB contamination may also be anomalously high in any particular field, and this should also be investigated. The purpose of this paper is to investigate and correct the effect of these contaminations in the SZE signals measured from the first-year AMiBA observation, so as to provide unbiased SZE estimations for further science investigations in our companion papers.

We do not, here, consider the effects of ground pick-up and other technical issues to do with the observing technique — the two-patch method used to deal with such problems is discussed elsewhere (Lin et al. 2009, Wu et al. 2009). Rather we investigate the CMB and Galactic emission environment (using data from the Wilkinson Microwave Anisotropy Probe, WMAP) and the known cm-wave radio source population (using source lists from several surveys) to estimate their effect on SZE results for the six clusters of galaxies observed by AMiBA. We describe our SZE analysis in Sec. 2, and discuss the errors in the presence of the sources of contamination in Sec. 3. A summary of the final results is given in Sec. 4.

## 2. SZE Flux Analysis

Between April and August 2007 AMiBA observed six galaxy clusters, A1689, A1995, A2142, A2163, A2261 and A2390. These SZE data have been combined with X-ray information in the literature to estimate the Hubble constant (Koch et al. 2009b) and study the scaling relation (Huang et al. 2009). In combination with Subaru weak lensing data they have also been used to study the gas fraction (Umetsu et al. 2009). Crucial to this work is the proper estimation of the errors on the measured SZE in the presence of contaminating signals. In this section we describe

the basic analysis used to measure the key parameters of the cluster SZE.

The fundamental observable for AMiBA is the visibility, which is the Fourier transform of the sky intensity multiplied by the primary beam or aperture function:

$$\mathcal{V}(u_j, v_j) = g \int dx dy A(x, y) \Delta I(x, y) e^{-2\pi i(ux+vy)}, \quad (1)$$

where  $g$  is a gain factor, which can be measured by calibration,  $(u, v)$  are components of the spatial separation vector of two antennas in the array in units of the observing wavelength,  $\lambda$ ,  $A(x, y)$  is the primary beam pattern,  $(x, y)$  are two components of angular position on the sky, measured relative to the phase centre (taken here to coincide with the pointing centre) and  $\Delta I(x, y)$  is the distribution of surface brightness of the sky. Here we have approximated the sky as being flat. Details of conversion from correlator data to visibilities is described in Wu et al. (2009).

Given the SZE flux density in the sky, one can calculate the visibility from equation (1). The SZE flux density of a cluster depends on observing frequency, the physics of the cluster atmosphere (gas temperature and density distributions, peculiar velocity, etc), and the angular diameter distance,  $D_A$ . If we adopt a spherical isothermal  $\beta$ -model (Cavaliere & Fusco-Femiano 1976), the visibilities measured by an interferometer are

$$\mathcal{V}_{\text{SZE}}(u, v) = I_0 \int dx dy A(x, y) \left(1 + \frac{\theta^2}{\theta_0^2}\right)^{-\frac{3}{2}\beta + \frac{1}{2}} \times e^{-2\pi i(ux+vy)}, \quad (2)$$

where  $I_0$  is the central surface brightness of the SZE,  $\theta^2 = (x - x_0)^2 + (y - y_0)^2$ ,  $(x_0, y_0)$  gives the sky position of the centre of the cluster,  $\theta_0$  is the angular core radius of the cluster, and  $\beta$  is the shape parameter.

For much of the SZE science (Birkinshaw 1999) that we can currently tackle with AMiBA we need to estimate the quantity  $I_0$  by fitting the model in equation (2) to the measured visibilities. AMiBA visibilities are estimated in a process that includes conversion from the wide-band, 4-lag, correlated analog signal into visibilities in two frequency channels (Wu et al. 2009) after tests on the quality of the data as discussed by Nishioka et al. (2009). In the hexagonal close-packed configuration used for observing the six clusters, the seven elements instantaneously yield 21 baseline vectors of three different lengths. Eight platform rotation angles relative to the pointing center are used to improve the  $u - v$  sampling.

In Figure (1), we show the observed real and imaginary parts of the visibilities as a function of multipole  $\ell = 2\pi(u^2 + v^2)^{1/2}$ . The averaging in azimuth uses  $\sigma^{-2}$  noise weighting, and for each baseline length the information from the two frequency channels is combined.

We fit the visibility model in equation (2) by minimizing  $\chi^2$  with respect to  $I_0$  and the location  $(x_0, y_0)$  of the cluster center. Because of the limited coverage in  $\ell$ , the values of  $\beta$  and  $\theta_0$  can not be usefully constrained by our data so we use values from the literature, which are consistently used by our companion papers (Huang et al. 2009, Koch et al. 2009b, Wu et al. 2009).

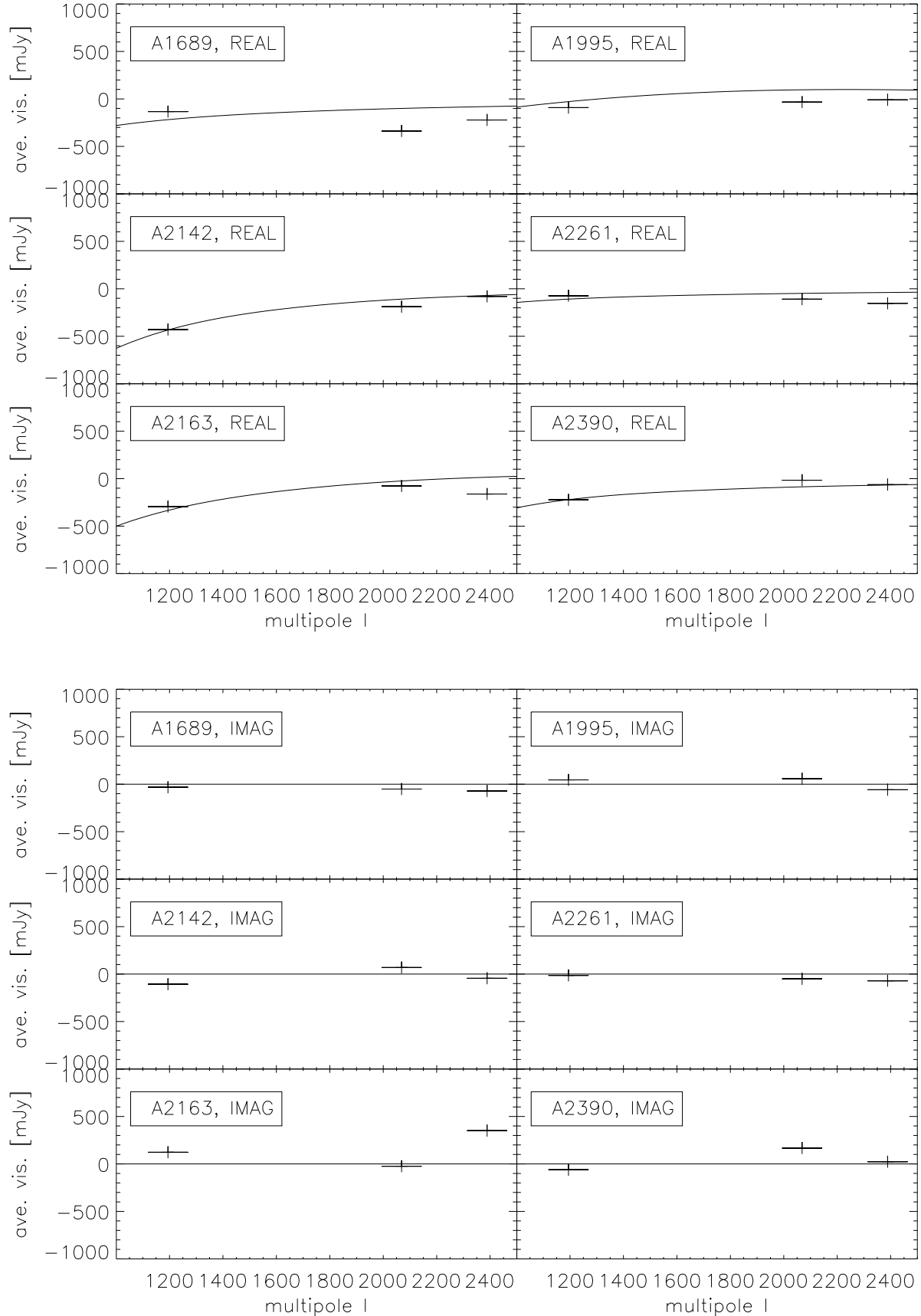


Fig. 1.— Averaged visibilities and best-fitting  $\beta$ -model profiles for the six AMiBA galaxy clusters. The data points show error bars based on the  $1\text{-}\sigma$  instrumental noise only. No contamination has been taken into account.

The fitted results for  $I_0$ ,  $x_0$ , and  $y_0$  for the clusters are given in Table 1. The errors were calculated from the Hessian matrix in the usual manner. The best-fit visibility profiles are shown with the data in Figure 1. At this stage no contribution to the errors from CMB or radio source confusion has been taken into account. These effects are the subject of the remainder of this paper.

### 3. Error Analysis

#### 3.1. Large-scale CMB and Galactic-emission contamination

WMAP has recently released full-sky temperature and polarization maps based on their five-year accumulated data. The angular resolution of WMAP varies from  $0.88^\circ$  to  $0.22^\circ$  over five bands from 23 to 94 GHz, and since the frequency range extends up to the AMiBA operating band, the WMAP data provide a good check on the level of CMB and Galactic contamination of the AMiBA data, although at lower angular resolution.

We use the CMB map produced by the Internal Linear Combination (ILC) method that is independent of both external data and assumptions about foreground emission, and estimate the Galactic foreground using the maps of synchrotron, free-free, and dust foregrounds produced by the Maximum Entropy Method (Gold et al. 2008). All four maps are smoothed to  $1^\circ$  scales, so that the principal indication that can be obtained is only whether there are unusually “hot” or “cold” spots near the clusters or trailing fields, and so whether there is likely to be additional noise power on the angular scales to which AMiBA is sensitive.

We find no strong Galactic contamination in any of the six clusters, with the total Galactic emission being typically an order of magnitude fainter than the CMB signal (Table 2). On the smaller angular scales to which AMiBA is sensitive, the Galactic emission will be even less important, since its power spectrum falls roughly as a power law,  $C_\ell \propto \ell^{-\gamma}$  with  $\gamma = 2.0 - 3.0$

Table 1. Best-fit values for  $I_0$  and offset of the cluster centres, with  $1\text{-}\sigma$  uncertainties ignoring the effects of contamination.

Cluster	$I_0$ $\times 10^5 \text{ Jy/sr}$	offset in RA arcmin	offset in Dec arcmin
A1689	$-2.24 \pm 0.44$	$-0.05 \pm 0.63$	$0.02 \pm 0.63$
A1995	$-3.38 \pm 0.63$	$4.41 \pm 0.76$	$0.38 \pm 0.68$
A2142	$-2.16 \pm 0.19$	$-0.64 \pm 0.42$	$0.19 \pm 0.41$
A2163	$-3.56 \pm 0.37$	$2.53 \pm 0.47$	$-2.36 \pm 0.53$
A2261	$-1.46 \pm 0.40$	$0.43 \pm 1.21$	$1.31 \pm 1.19$
A2390	$-2.42 \pm 0.36$	$0.60 \pm 0.81$	$-1.74 \pm 0.56$

(Tegmark et al. 2000). Here the power spectrum is defined as

$$C_\ell = \frac{1}{2\ell + 1} \sum_m \langle a_{\ell m}^* a_{\ell m} \rangle \quad (3)$$

with  $a_{\ell m}$  the expansion coefficient of temperature field on the spherical harmonics. Thus we expect that Galactic contamination will be two orders of magnitude fainter than the primordial CMB signal as seen in the WMAP data.

We summarize the CMB surface brightness fluctuations in the clusters and trailing fields on the angular scale of the clusters, based on the WMAP ILC image, in Table 1. The values range up to  $\sim 25$  kJy/sr ( $\sim 100$   $\mu$ K in temperature units). The level of primordial contamination at the degree scale is suppressed by the 45-arcminute-separated two-patch subtraction technique, but nevertheless, we might expect elevated levels of CMB noise in fields with large degree-scale signals. This is consistent with the observed deviations from the expected visibility curves for the most contaminated clusters, A1689 and A2390.

### 3.2. Small-scale CMB and Galactic-emission estimation

Given the statistical properties of the CMB and Galactic emission, we are able to estimate the rms fluctuations on each baseline. Because of the two-patch observing strategy, we rewrite equation 1 as

$$\begin{aligned} \mathcal{V}(u_j, v_j, x_p, y_p) &= \int dx dy A(x - x_p, y - y_p) \Delta I(x, y) \\ &\quad \times e^{-2\pi i(u(x-x_p) + v(y-y_p))} \\ &= \int dudv \tilde{A}(u_j - u, v_j - v) a(u, v) \\ &\quad \times e^{2\pi i(u(x-x_p) + v(y-y_p))}, \end{aligned} \quad (4)$$

where  $(x_p, y_p)$  is the pointing center of the corresponding field, and  $a(u, v)$  is the Fourier transform of surface brightness of the sky. The two-point correlation function of  $a(\mathbf{u})$  is diagonal because of

Table 2. Large-scale CMB and Galactic emission ( smoothed to  $1^\circ$  scales).

Cluster	CMB(lead;trail) $\times 103\text{Jy/sr}$	Galactic(lead;trail) $\times 103\text{Jy/sr}$
A1689	+24.1; +22.3	0.0; 0.0
A1995	– 5.6; +14.0	0.0; 0.0
A2142	+ 8.5; +14.8	0.0; 0.0
A2163	+17.2; – 4.3	1.1; 7.3
A2261	– 0.2; + 4.2	0.5; 0.4
A2390	–25.2; –20.7	4.0; 1.4

the rotation invariant

$$\langle a(\mathbf{u})a(\mathbf{w}) \rangle = C_{\mathbf{u}} \delta^{(2)}(\mathbf{u} - \mathbf{w}), \quad (5)$$

where  $C_{\mathbf{u}} = (\partial B_{\nu}/\partial T)^2 C_{\ell}$  and  $\partial B_{\nu}/\partial T$  converts from temperature to intensity. We have adopted the flat-sky approximation, which is valid for AMiBA, so that  $\ell = 2\pi\mathbf{u} = 2\pi\sqrt{u^2 + v^2}$ .

The rms fluctuation in each baseline then is

$$\begin{aligned} \langle \mathcal{V}^2(u_j, v_j) \rangle = & \int du dv \tilde{A}^2(u_j - u, v_j - v) C_{\ell} \\ & \times \{1 - \cos[2\pi(u\Delta x + v\Delta y)]\}, \end{aligned} \quad (6)$$

where  $\tilde{A}$  is the Fourier transform of the primary beam,  $(\Delta x, \Delta y)$  is the separation of the clusters and trailing fields (about 45 arcminutes in most of our data). Since the universe is isotropic, we put  $\Delta x = 45$  and  $\Delta y = 0$  arcminutes when we calculate the rms fluctuation.

For the Galactic emission, we use the middle-of-the-road (MID) foreground model in Tegmark et al. 2000, which is intended to be realistic but conservative. We show the expected fluctuation from three Galactic emission components in Figure 2. The Galactic emission lies about two orders of magnitude below the contribution from the CMB. Other models in Tegmark et al. 2000 change the results by less than factor two. These results are consistent with what we expected in previous sub-section. Therefore, we ignore the contribution from Galactic emission in what follows.

The CMB surface brightness fluctuations expected for a  $\Lambda$ CDM model with the cosmological parameters estimated from the WMAP 5-year data alone (Dunkley et al. 2008) contribute uncertainties of 80.6, 20 and 11.4 mJy for the three averaged AMiBA baselines and exceed the instrument noise for all baselines in all six clusters.

To estimate the error in  $I_0$  from CMB anisotropies, we repeat the fitting of Sec. 2 for 500 simulated CMB skies where the CMB anisotropies have a power spectrum based on the cosmological parameters from the combination of five-year WMAP data. For each simulation we subtract the simulated CMB visibilities from the data and fit  $I_0$ , assuming that the central positions in Table 1 are unchanged. Our results for the noise introduced in the values of  $I_0$ ,  $\sigma_{\text{CMB}}$ , are shown in Table 3.

Table 3. Error and offset of  $I_0$  estimates from CMB and radio sources. The errors and offset are computed for each individual contaminant. The error on the final  $I_0$  is the total noise, including instrument noise, CMB, and radio sources.

Cluster	$\sigma_{\text{CMB}}$ $\times 10^5 \text{ Jy/sr}$	source offset $\times 10^5 \text{ Jy/sr}$	final $I_0$ $\times 10^5 \text{ Jy/sr}$
A1689	0.53	$-0.16 \pm 0.17$	$-2.40 \pm 0.71$
A1995	1.02	$+0.28 \pm 0.27$	$-3.10 \pm 1.22$
A2142	0.30	$-0.24 \pm 0.12$	$-2.40 \pm 0.37$
A2163	0.47	$-0.01 \pm 0.13$	$-3.16 \pm 0.61$
A2261	0.77	$-0.88 \pm 0.24$	$-2.34 \pm 0.90$
A2390	0.61	$-0.51 \pm 0.31$	$-2.93 \pm 0.77$

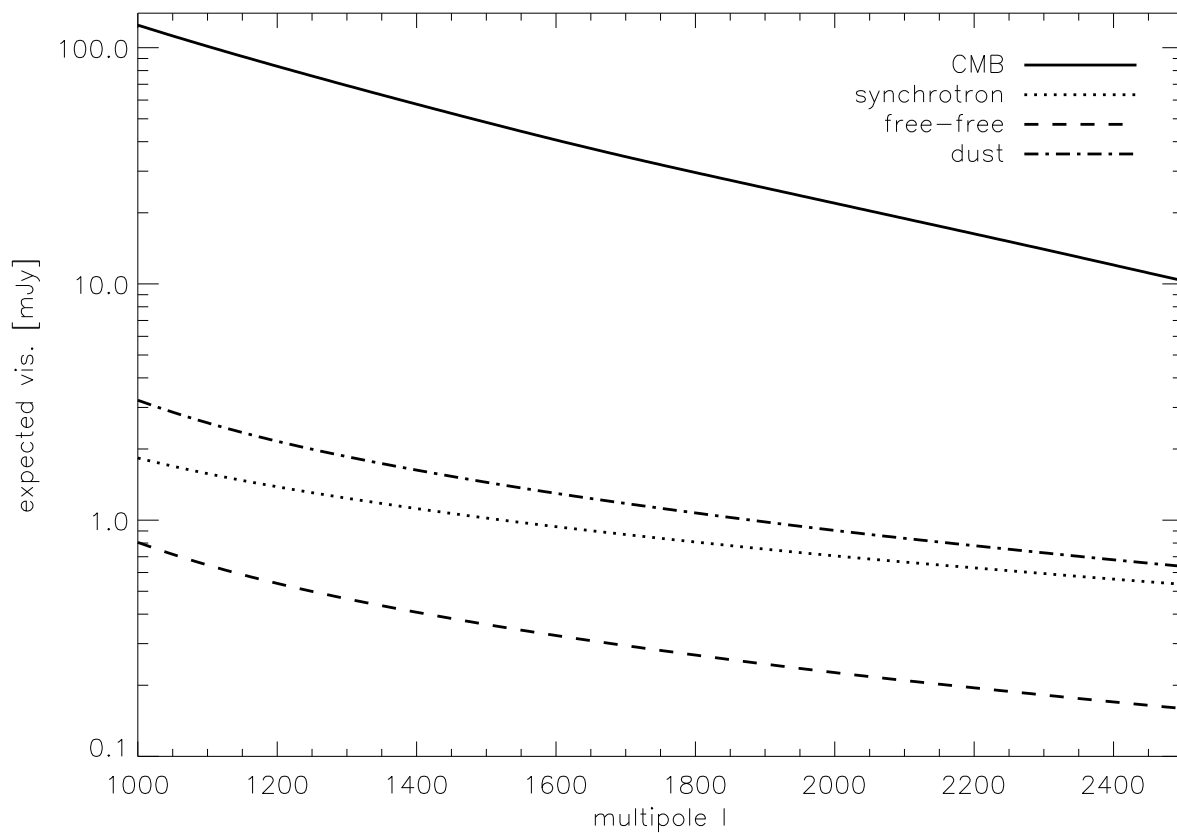


Fig. 2.— Expected response from CMB(solid) and synchrotron(dot), free-free(dashed), dust(dot-dashed) emission.

### 3.3. Foreground Point Sources

The emission from discrete sources will reduce the size of the SZE at 94 GHz if those sources are concentrated towards the target cluster, but can cause an increase in the measured value of  $I_0$  if they are located in the trailing field (or lie in negative sidelobes of the synthesized beam). Since we expect to see more radio sources towards the clusters, the measured SZE will normally be an underestimate of the true value (Coble et al. 2007).

Corrections for point source contamination can often be made by combining arcminute-resolution SZE data with high-resolution data (see, e.g., Lancaster et al. 2005, Udomprasert et al. 2008). However, such supporting data are not available for AMiBA. Because the point source population at 90 GHz is also poorly known, it is challenging to estimate the degree of contamination. Thus we take the following approaches.

In assessing the contributions from known sources, we use the 4.85-GHz GB6 and PMN catalogs (Gregory et al. 1996; Griffith et al. 1995). The GB6 survey covered declinations  $0^\circ < \delta < +75^\circ$  to a flux density limit  $S_{4.85} = 18$  mJy. The four declination bands in the PMN survey from  $-88^\circ < \delta < +10^\circ$  and have flux density limits  $S_{4.85} = 20 - 70$  mJy. We estimate the contamination for fainter sources with significant low-frequency emission using the NVSS catalog at 1.4 GHz (Condon et al. 1998), which is complete for  $\delta > -40^\circ$  with flux density limit 2.5 mJy. In each case we investigate the radio environments of the clusters by extracting radio sources within  $20'$  of clusters and trailing fields. These sources are summarized in Table 4. We also estimate their flux densities at AMiBA’s operating frequency by simply assuming power law spectra of the form  $S_\nu \propto \nu^\alpha$  with  $\alpha$  the spectral index.

In each field we find 20 – 30 objects in the NVSS and from zero to three objects in the GB6 or PMN lists. Most of these sources are too faint to affect the AMiBA data, but two GB6 sources are bright enough to cause problems. A source with  $S_{4.85} = 192$  mJy lies  $14'3$  from the center of the trail patch of A2261. The other has  $S_{4.85} = 294$  mJy and lies  $18'6$  from the center of A2390. However, the VLA calibrator catalog suggests that both sources have falling spectra above 8 GHz, with predicted 94 GHz flux densities of  $130 \pm 20$  and  $90 \pm 20$  mJy if the high-frequency spectra are power laws and variability is not important. Both sources lie beyond the half-power point of the AMiBA beam (at the 30% and 13% levels for offsets of  $14'3$  and  $18'6$ , respectively; Wu et al. 2009). We fit the value of  $I_0$  with the spectral indices  $\alpha$  of all of the sources listed at 4.85-GHz for these two clusters. We found spectral indices of  $-0.02 \pm 0.13$  (implying a 3-mm flux density  $S = 203_{-67}^{+100}$  mJy) and  $0.04 \pm 0.03$  (implying a 3-mm flux density  $S = 328_{-198}^{+500}$  mJy) for the problem sources in the trail patch of A2261 and the main A2390 field, respectively. Although these sources are not detected, we expect them to significantly affect the fitted value of  $I_0$ .

None of the catalogued point sources is detected by AMiBA (at an rms sensitivity of 50 mJy) in the residual maps formed by subtracting the best-fit cluster SZE models from the visibility data. Therefore we adopt a statistical method of estimating the contamination from the known point sources. This involves simultaneously estimating the spectral indices of known sources from 4.85

Table 4. Radio sources in the cluster fields from 6 cm catalogs.

Cluster	RA (J2000)	Dec (J2000)	$S_{6\text{ cm}}$ <sup>a</sup> mJy	$S_{20\text{ cm}}$ <sup>b</sup> mJy	$S_{3\text{ mm}}$ <sup>c</sup> mJy	$\alpha$	$\Delta\theta$ arcmin
A1995	14 52 50.8	57 46 58.0	28	25	36.0	0.08	16.0
	14 52 33.8	57 53 48.0	21	53	2.3	-0.75	9.3
	14 52 16.9	58 13 28.0	17	53	1.1	-0.91	11.5
	14 57 41.2	57 57 03.5	60	182	4.3	-0.89	12.7*
	14 57 56.3	57 44 47.1	56	81	23.0	-0.3	20.0*
A2142	15 58 13.0	27 16 22.4	39	107	3.5	-0.81	3.2
	15 58 34.9	27 30 45.0	21	–	–	–	17.4
	16 02 59.6	27 21 35.0	83	364	2.4	-1.19	6.2*
A2163	16 15 54.6	-6 08 44.0	42	–	–	–	5.3
	06 18 40.8	-6 17 18.0	56	–	–	–	10.0*
A2261	17 22 24.2	32 01 24.3	56	126	8.1	-0.65	6.3
	17 26 19.4	32 19 19.5	37	104	3.2	-0.82	15.2*
	17 26 20.5	32 01 26.0	29	–	–	–	11.7*
	17 26 35.3	32 13 30.0	192	126	522	0.34	14.3*
A2390	21 54 40.9	17 27 53.0	294	294	294	0	18.6
	21 57 05.4	17 51 15.0	81	270	4.6	-0.97	10.5*
	21 56 43.8	17 22 49.0	41	136	2.3	-0.93	19.1*

<sup>a</sup>PMN and GB6 (Gregory et al. 1996; Griffith et al. 1995)

<sup>b</sup>NVSS catalogs (Condon et. al. 1998)

<sup>c</sup>Extrapolation to AMiBA frequency by power law

\*Radio sources located in the trailing fields

to 94 GHz and the value of  $I_0$  for the cluster. We do not use any prior on the spectral indices because the results are very sensitive to the assumed distribution. We cannot apply this method for the NVSS sources because the problem is generally underdetermined: there are too many NVSS sources to fit.

We account for the contribution of NVSS sources using Monte Carlo simulations. In each of 500 runs, we pick a set of spectral indices for the sources from the WMAP distribution, predict the 94 GHz flux densities (forcing no source to exceed the GB6 or PMN limit), and estimate the visibilities. We then subtract these simulated visibilities from the AMiBA data, and re-fit the value of  $I_0$  and the spectral indices of the sources in the 4.85-GHz catalogs. We expect this to be an upper limit to the level of confusion noise from foreground and background radio sources not represented in the source surveys to date.

The effects of point sources on the value of  $I_0$  are summarized in Table 3. The value of  $I_0$  increases by less than its random error in the four clusters without strong 4.85-GHz contaminating sources, but significant changes are seen for A2261 and A2390. In these cases follow-up observations of the sources are highly desirable. The additional noise contributed by the population of point sources is, however, always considerably less than the noise from CMB anisotropies.

#### 4. Discussion and Conclusion

The levels of contamination estimated in this paper are summarized in Table 3. Except for A2261, the dominant source of confusion is the primordial anisotropy of the CMB, which adds noise at the level of 13 – 50% of the value of  $I_0$ , exceeding the AMiBA system noise in every case. Galactic foreground emission is always negligible.

Known point sources affect the amplitudes of the SZE of the clusters by less than the combined system and CMB noises in each case except A2261, but ignoring the sources would systematically bias the estimates of  $I_0$  because there are more radio sources towards the clusters than in the background fields. A2261 suffers particularly substantial contamination. When we fit the spectral indices for sources in the 4.85-GHz catalog only, we find that  $I_0 = -(1.81 \pm 0.43) \times 10^5$  Jy/sr. A comparison with Table 3 shows that faint sources in the NVSS catalog produce a non-negligible  $I_0$  offset.

Several other workers have reported on the discrete source environments of these clusters. Reese et al. (2002) report on radio sources at 28.5 and 30 GHz for A1689, A1995, A2163 and A2261. All of these sources are in NVSS, but none is bright enough at 5 GHz to appear in the GB6 or PMN catalogs: the brightest is a 10 mJy source in A2261. The VSA source-subtractor also reports on sources in A2142 (Lancaster et al. 2005): all are included in the NVSS catalog, and the contamination that they generate is small (less than 3% of  $I_0$ ).

Tucci et al. (2008) have studied radio source spectra from 1.4 – 33 GHz. They found that, in

general, the spectra are not well described by a single power law: the low-frequency spectra are usually steeper than the high-frequency spectra. Spectral index studies from 1.4 – 28.5 GHz (e.g., Coble et al. 2007) and 23 – 94 GHz (Wright et al. 2008) support this behaviour. Our study, which extrapolated from 1.4 GHz (or 4.85 GHz) to 94 GHz using the WMAP spectral index distribution may overestimate the contamination from radio sources.

Our best estimates of  $I_0$ , taking contamination into account, are shown in the last column of Table 3, where we calculate the total uncertainty by summing the contributions of instrument noise, CMB and point sources in quadrature. These values are further used in the science analysis of our companion papers.

We acknowledge the extensive use we have made of data from the WMAP satellite, and thank Dr. L. Chiang for fruitful discussions on Galactic emission and the WMAP data. We also appreciate discussions with Drs N. Aghanim and S. Matsushita on radio source properties. Support from the STFC for MB is acknowledged. This work is partially supported by the National Science Council of Taiwan under the grant NSC97-2112-M-032-007-MY3.

## REFERENCES

- Birkinshaw, M., 1999, *Phys. Rep.*, 310, 97
- Cavaliere, A., & Fusco-Femiano, R., 1976, *A&A*. 49, 137
- Chen, M.-T., et al., 2009, *ApJ* in press (this issue)
- Condon, J. J., Cotton, W. D., Greisen, E. W., Yin, Q. F., Perley, R. A., Taylor, G. B., & Broderick, J. J. 1998, *AJ*, 115, 1693
- Coble, K., Bonamente, M., Carlstrom, J. E., Dawson, K., Hasler, N., Holzapfel, W., Joy, M., LaRoque, S., Marrone, D. P., Reese, E. D. 2007, *AJ*, 134, 897
- Dunkley, J. et al., 2008, submitted to *ApJS*
- Gold B., et al., 2009, *ApJS*, 180, 265
- Gregory, P. C., Scott, W. K., Douglas, K., Condon, J. J., 1996, *ApJS*, 103, 427
- Griffith, Mark R., Wright, Alan E., Burke, B. F., Ekers, R. D., 1995, *ApJS*, 97, 347
- Ho, P.T.P., et al., 2009, *ApJ* in press (this issue)
- Huang, C., et al. 2009, submitted to *ApJ* (this issue)
- Koch, P. M., et al. 2009a, *ApJ* in press (this issue)
- Koch, P. M., et al. 2009b, submitted to *ApJ* (this issue)

- Lancaster, K. et al., 2005, *Mon. Not. R. Astron. Soc.*, 359, 16
- Lin, K.Y. et al. 2009, *ApJ* in press (this issue)
- Nishioka, H., et al., 2009, *ApJ* in press (this issue)
- Reese, E. D., Carlstrom, J. E., Joy, M., Mohr, J., & Grego, L., 2002, *ApJ.*, 581, 53
- Sunyaev, R. A., & Zel'dovich, Y. B., 1972, *Comments Astrophys. Space Phys.*, 4, 173
- Tegmark, M., Eisenstein, D. J., Hu, W., de Oliveira-Costa, A., 2000, *ApJ*, 530, 133
- Tucci, M. et al., 2008, *MNRAS*, 386, 1729
- Udomprasert, P. S., Mason, B. S., Readhead, A. C. S., and Pearson, T. J., 2004, *ApJ*, 615, 63
- Umetsu, K. et al. 2009, *ApJ* in press (this issue)
- Wright, E. L. et al. 2008, submitted to *ApJS*
- Wu, J. H. P. et al., 2009, *ApJ* in press (this issue)